Available online www.worldscientificnews.com

World Scientific News

An International Scientific Journal

WSN 209 (2025) 19-32 EISSN 2392-2192

Synthesis of coumarin pyrazole derivatives chelate complexes with Neodymium (III) and Clioquinol: as potential antimicrobial agent.

H. G. Solanki[1] | G. J. Kharadi [1*]

[1,1*]Navjivan Science College, Dahod, Gujarat, India,

Shri Govind Guru University, Godhra, Gujarat, India.

*Corresponding author

ABSTRACT

A viable tactic to counteract drug-resistant bacteria is the creation of metal-based antimicrobial agents. Here, we present the synthesis and design of new coumarin–pyrazole compounds together with their coordination complexes with clioquinol and neodymium (III). After being produced via condensation, the ligands complexed with Nd (III) ions in the presence of Clioquinol to form stable chelates. Key bonding interactions were clarified, and effective coordination was validated by structural analysis employing FT-IR, NMR, and mass spectrometry (MS). With noticeably lower minimum inhibitory concentrations than the free ligands or metal salts alone, the resultant complexes demonstrated improved antibacterial activity against a spectrum of bacterial and fungal species. These findings point to a metal–ligand interaction-driven synergistic antibacterial mechanism that presents a viable framework for the creation of next-generation antimicrobial drugs.

Keywords: Coumarin-pyrazole derivative, Neodymium metal complex, Clioquinol.

(Received 24 September 2025; Accepted 15 October 2025; Date of Publication 9 November 2025)

1. INTRODUCTION

The investigation of coordination compounds formed through the complexation of coumarin derivatives with various metal ions has attracted considerable attention in recent years due to their promising biological and chemical properties [1]. Coumarin, or 2H-chromene-2-one, is an aromatic organic compound comprising a benzopyrone core structure formed by the fusion of a benzene ring with an α-pyrone ring [2]. Structural modifications at specific positions, particularly the third and fourth carbons, lead to the generation of benzo[c]coumarin and its derivatives, which can be derived from natural plant sources [3] or synthesized via chemical methods [4]. These derivatives exhibit a broad range of pharmacological activities, including antidyslipidemic, anti-inflammatory, vasodilatory, antimicrobial, antithrombotic, anti-mutagenic, antioxidant, antiallergic, antiviral, anticarcinogenic, and antitumor properties [5–7].

In the field of synthetic organic chemistry, the coumarin nucleus has been widely modified by fusing it with various heterocyclic moieties such as pyridine, furan, pyrazole, oxazole, and triazole. These modifications, particularly at the lactone ring, are designed to enhance biological activity and increase structural diversity [8,9]. The resulting hybrid heterocyclic systems often exhibit improved therapeutic potential, making them attractive targets for drug design and development.

Clioquinol (5-chloro-7-iodo-8-quinolinol), a halogenated hydroxyquinoline compound, has been extensively studied due to its broad-spectrum antimicrobial and antiparasitic properties. Historically used as an antifungal and antiprotozoal agent, clioquinol has also demonstrated potential in anticancer and neuroprotective therapies [10,11]. Its ability to chelate metal ions such as copper, zinc, and iron plays a key role in its pharmacological action [12]. Clioquinol and its derivatives can act as effective ligands in coordination chemistry due to the presence of both nitrogen and hydroxyl donor atoms, which facilitate stable complex formation with various metal ions [13].

Clioquinol-based metal complexes have gained increasing interest in recent years due to their enhanced biological activities compared to the parent compound. These include improved antimicrobial, anticancer, and antioxidant properties, often attributed to the synergistic effect between the metal center and the bioactive ligand [14]. Additionally, metal coordination can modulate the pharmacokinetic behaviour of clioquinol, making such complexes promising candidates for drug development and biomedical applications [15].

In this study, a novel coumarin-based ligand, 3-(4-(1,4-diphenyl-1H-pyrazol-3-yl)-6-phenylpyridin-2-yl)-2H-chromen-2-one, was synthesized from a 1-(2-oxo-2-(2-oxo-2H-chromen-3-yl)ethyl)pyridin-1-ium bromide and (E)-3-(1,3-diphenyl-1H-pyrazol-4-yl)-1-phenylprop-2-en-1-one precursor, ammonium acetate, and ammonia. Additionally, clioquinol ligands were purchasing and employed for complexation with neodymium (III) salts, yielding novel neodymium coordination complexes.

The synthesized ligands and their Nd (III) complexes were characterized using a suite of analytical and spectroscopic techniques, including ^{1}H-NMR, infrared (IR) spectroscopy, thermogravimetric analysis (TGA), elemental analysis, and fast atom bombardment (FAB) mass spectrometry. Magnetic susceptibility measurements indicated that the neodymium complexes adopt an octahedral geometry.

Furthermore, the antimicrobial activities of the ligands and their neodymium complexes were assessed using the agar well diffusion method against selected bacterial and fungal strains. The results revealed that the metal complexes exhibited superior antimicrobial activity compared to the free ligands and neodymium salt, with activity levels approaching those of standard antimicrobial agents.

2. EXPERIMENTAL

Materials and Methodes

All chemicals and reagents used in this study were of analytical grade and employed without further purification. Salicylaldehyde, benzaldehyde, acetophenone, 4-methylacetophenone,4-methoxyacetophenone, 4-methoxyacetophenone, and ethyl acetoacetate, $POCl_3$ were obtained from Sigma-Aldrich. Additional reagents, including piperidine, pyridine, diethyl ether, ammonium acetate, chloroform, toluene, and bromine, were also sourced from commercial suppliers and used as received. Neodymium (III) nitrate hexahydrate ($Nd(NO_3)_3 \cdot 6H_2O$) was used as the metal precursor for the synthesis of the neodymium complexes. All solvents employed were of reagent grade and were freshly distilled when required. The syntheses were conducted under standard laboratory conditions unless otherwise specified.

Preparation of Ligands

The ligand (L_1 – L_9) synthesized using modified method literature procedure [14]. 3-(4-(1,4-diphenyl-1H-pyrazol-3-yl)-6-phenylpyridin-2-yl)-2H-chromen-2-one (0.003 mol) was dissolve in glacial acetic acid (15 mL) and stirred with ammonium acetate (0.003 mol) at room temperature. A solution of pyrazolyl chalcone (0.003 mol) in acetic acid (15mL) was added over 15minutes. The mixture was stirred for 1 hour at room temperature. Them reflux at 140 ^{0}C for 121 hours. After cooling, the mixture was poured in the ice-cold water (75mL), and the crude product was extracted with chloroform. The organic layer was washed with sodium bicarbonate and water, dried, and concentrated. The residue was purified by column chromatography using ethyl-acetate-pet. Ether, 2:8 ratio as the eluent. The final products L_1 – L_9) were recrystallized form chloroform– hexane mixture.

Scheme 1. Synthesis of Coumarin-Pyrazole Derivative.

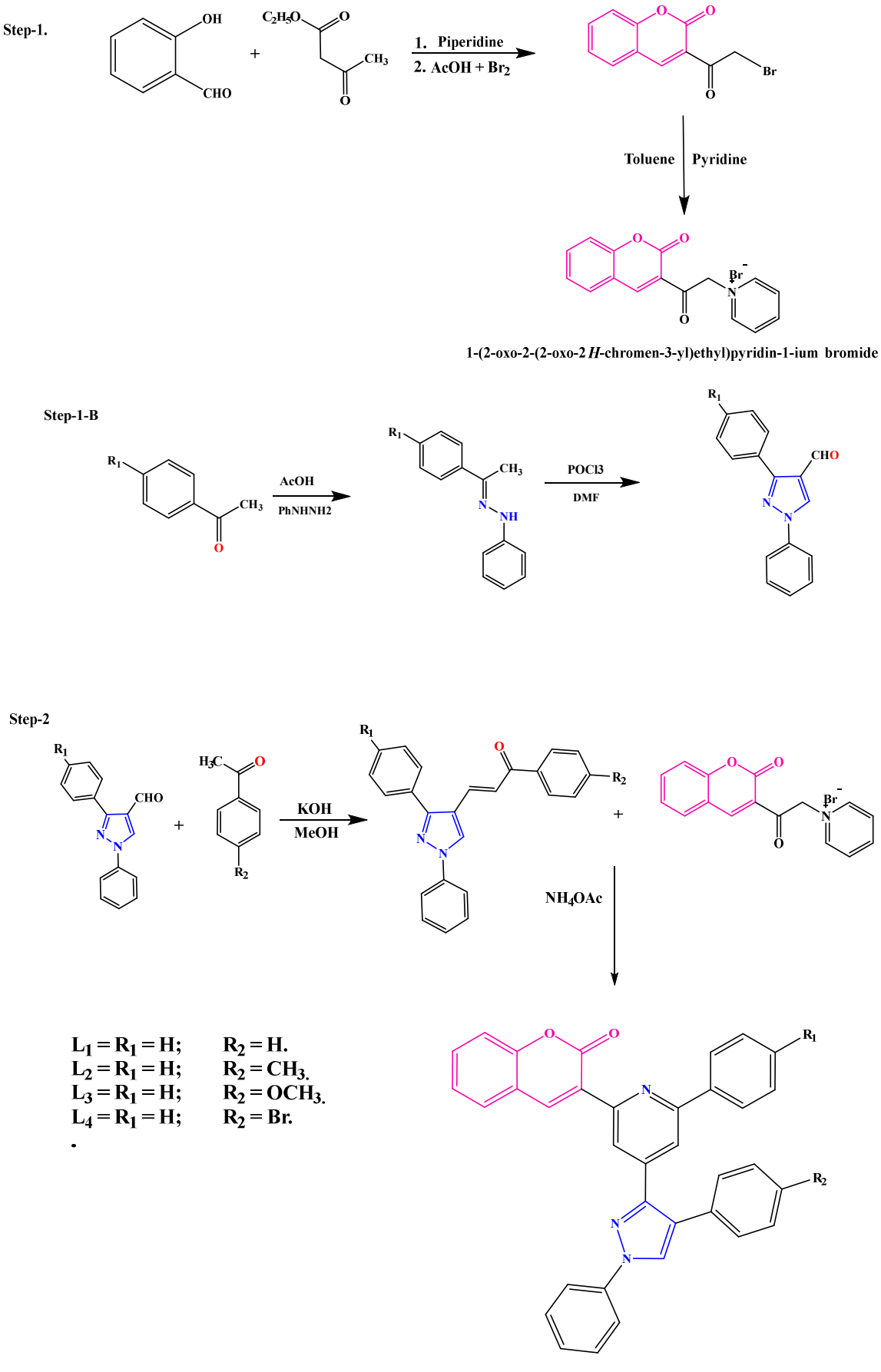

Table 1. Physical and elemental analysis of Coumarin – pyrazole derivatives (L_1 – L_4).

Ligand	Molecular formula	Colour	Molecular weight Found (Cal.)	% Analysis found		
				C	H	N
L_1	$C_{35}H_{23}N_3O_2$	Yellow	517.59 (517.65)	81.22 (81.20)	4.48 (4.45)	8.12 (8.10)
L_2	$C_{36}H_{25}N_3O_2$	Yellow	531.62 (531.65)	81.34 (81.32)	4.74 (4.72)	7.90 (4.87)
L_3	$C_{36}H_{25}N_3O_3$	Yellow	547.61 (547.65)	78.96 (78.94)	4.60 (4.59)	7.67 (7.65)
L_4	$C_{35}H_{22}BrN_3O_2$	Pale – yellow	595.09 (595.13)	70.48 (70.45)	3.72 (3.70)	7.04 (7.02)

- **3-(4-(1,4-diphenyl-1H-pyrazol-3-yl)-6-phenylpyridin-2-yl)-2H-chromen-2-one (L_1):**
  Yield: 64%, m.p. 218 - 220°C,
  IR (cm^{-1}): 3040 (aromatic C–H), 1730 (C=O, 8-lactone of coumarin), 1595, 1490 (aromatic C=C and C=N), 835 (p-disubstituted benzene C–H bending), 755 (monosubstituted benzene C–H bending).

  ^{1}H NMR (δ, ppm, $CDCl_3$): 7.25–7.87 (19H, m, aromatic protons), 8.33 (1H, s, pyrazole C5–H), 8.49 (1H, s, pyridine C3′–H), 8.99 (1H, s, coumarin C4–H).

  ^{13}C NMR (δ, ppm, $CDCl_3$): 21.3 (CH_3), 116–130 (aromatic/CH), 132–143 (quaternary/aromatic C), 151–160 (C=O, C=N, other quaternary C)

- **3-(6-phenyl-4-(1-phenyl-4-(p-tolyl)-1H-pyrazol-3-yl) pyridin-2-yl)-2H-chromen-2-one (L_2):**
  Yield: 65%, m.p : 212 - 214°C
  IR (cm^{-1}): 3040 (aromatic C–H), 1730 (C=O, 8-lactone of coumarin), 1595, 1490 (aromatic C=C and C=N), 835 (p-disubstituted benzene C–H bending), 755 (monosubstituted benzene C–H bending).

  ^{1}H NMR (δ, ppm, $CDCl_3$): 2.42 (3H, s, CH_3), 7.25–7.87 (19H, m, aromatic protons), 8.33 (1H, s, pyrazole C5–H), 8.49 (1H, s, pyridine C3′–H), 8.99 (1H, s, coumarin C4–H).

  ^{13}C NMR (δ, ppm, $CDCl_3$): 21.3 (CH_3), 116–130 (aromatic/CH), 132–143 (quaternary/aromatic C), 151–160 (C=O, C=N, other quaternary C)

- **3-(4-(4-(4-methoxyphenyl)-1-phenyl-1H-pyrazol-3-yl)-6-phenylpyridin-2-yl)-2H-chromen-2-one (L_3):**
  Yield: 84%, m.p.: 222 - 224°C

  IR (cm^{-1}): 3045 (aromatic C–H), 1270, 1040 (asymmetric and symmetric C–O–C stretching), 775 (monosubstituted benzene C–H bending), 835 (p-disubstituted benzene C–H bending), 1730 (C=O stretching of 8-lactone of coumarin), 1595, 1490 (aromatic C=C and C=N).

  ^{1}H NMR (δ, ppm, $CDCl_3$): 3.86 (3H, s, OCH_3), 6.96–7.85 (19H, m, aromatic protons), 8.31 (1H, s, pyrazole C5–H), 8.44 (1H, s, pyridine C3′–H), 8.95 (1H, s, coumarin C4–H).

  ^{13}C NMR (δ, ppm, $CDCl_3$): 55.37 (OCH_3), 114–130 (aromatic/CH), 131–143 (quaternary/aromatic C), 151–160 (C=O, C=N, other quaternary C).

- **3-(4-(4-(4-bromophenyl)-1-phenyl-1H-pyrazol-3-yl)-6-phenylpyridin-2-yl)-2H-chromen-2-one (L_4):**
  Yield: 54%, m.p.: 152 - 154°C

  IR (cm^{-1}): 3065 (aromatic C–H), 760 (monosubstituted benzene C–H bending), 820 (p-disubstituted benzene C–H bending), 1735 (C=O stretching of 8-lactone of coumarin), 1600, 1475 (aromatic C=C and C=N).

  ^{1}H NMR (δ, ppm, $CDCl_3$): 7.36–7.91 (19H, m, aromatic protons), 8.34 (1H, s, pyrazole C5–H), 8.52 (1H, s, pyridine C3′–H), 8.99 (1H, s, coumarin C4–H).

  ^{13}C NMR (δ, ppm, $CDCl_3$): 116–130 (aromatic/CH), 132–143 (quaternary/aromatic C), 151–159 (C=O, C=N, other quaternary C).

Synthesis of Neodymium (III) Complexes (C_1 – C_4)

To synthesize a neodymium (III) complex featuring clioquinol and a coumarin derivative, clioquinol is dissolved in ethanol under gentle heating, while the coumarin– pyrazole derivative ligands (L_1 – L_4) is separately dissolved in ethanol, aided if needed by a base such as triethylamine. These ligand solutions are added sequentially to a stirred solution of neodymium (III) nitrate hexahydrate in ethanol (or ethanol/water). The mixture is refluxed for 4–6 hours at pH 6–7 (adjusted with triethylamine). After cooling, the reaction is chilled at ~4 °C overnight to rad – brown precipitate the complex (C_1 – C_7). The solid is then filtered, washed with cold ethanol, and thoroughly dried (vacuum or ~60 °C oven) [15]. The common rection procedure scheme is depicted in Scheme 2. All complexes' physical and analytical data is filled in Table 2.

Scheme 2. Nd(III) complex synthesis (C_1 – C_4).

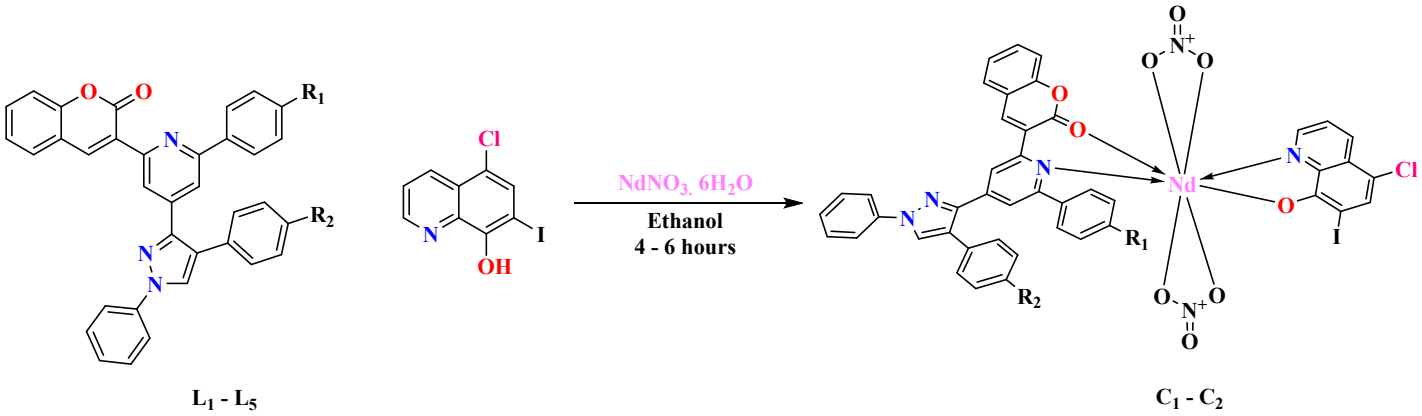

Table 2. Physical and analytical data of Nd(III) complexes.

Complex	Molecular Formula	Colour	Yield (%)	Molecular Weight	Melting Point (C)	% fond (required)			
						C	H	N	Nd
C_1	$C_{44}H_{27}Cl_3IN_4NdO_3$. 2H2O	Redis – brown	54%	1055.23	218 – 220	50.78	2.65	5.38	13.86
C_2	C45H29Cl3IN4Nd O3.2H2O	Redis – brown	65%	1069.26	212 – 241	51.24	2.81	5.31	13.67
C_3	C45H29Cl3IN4Nd O4.2H2O	Redis – brown	53%	1085.26	222 – 224	50.47	2.77	5.23	13.47
C_4	C44H26Cl3BrIN4 NdO3.2H2O	Redis – brown	53%	1134.13	152 – 154	47.20	2.38	5.00	12.88

3. RESULT

Table 1 provides the physical and elemental analysis data of ligand (L_1 – L_4) and Table 2 provides physical and analytical data complex (C_1 – C_4). The rection below represent the pathway for the formation of these complexes. The synthesized neodymium (III) Complexes were insoluble in most common organic solvent but showed moderate solubility in DMF and good solubility in DMSO.

Magnetic Properties of Nd(II) Complexes.

Table 3. Magnetic measurement data and electronic spectroscopy of neodymium (III) complexes (C_1 – C_4).

Complex	Transition range (cm^{-1})	Transition ($^4I_{9/2} \rightarrow {}^4F_{3/2}$) nm	μ_eff (B. M.)
C_1	11335	865	3.60
C_2	11490	825	3.62
C_3	11290	740	3.58
C_4	12010	770	3.65

IR Spectra

Table 4 present the significant infrared spectral bands recorded using KBr pellet and their corresponding assignment for the synthesized complexes. The synthesized neodymium (III) complexes. The υ(C=O) vibration band of ligand. When coumarin–pyridine and clioquinol act as ligands and coordinate with neodymium (III) (Nd^{3+}) ions, noticeable changes occur in their infrared (IR) spectra, particularly in regions associated with donor atoms. In the case of the coumarin–pyridine ligand, coordination primarily occurs through the carbonyl oxygen of the coumarin moiety and the nitrogen atom of the pyridine ring. This interaction leads to a shift of the carbonyl (C=O) stretching frequency from its typical range of 1700–1725 cm^{-1} to a lower region around 1670–1690 cm^{-1}, indicating involvement of the carbonyl group in coordination. Similarly, the C=N stretching frequency of the pyridine ring, originally around 1580–1600 cm^{-1}, shifts to a lower frequency region (approximately 1550–1580 cm^{-1}), suggesting bonding through the nitrogen atom. Additionally, new bands appear in the 400–600 cm^{-1} range, corresponding to the formation of Nd–O and Nd–N bonds.

For clioquinol, which is clioquinol, coordination occurs through the phenolic oxygen (after deprotonation) and the nitrogen atom of the quinoline ring. Upon binding with Nd^{3+}, the broad O–H stretching band typically observed around 3400 cm^{-1} diminishes or disappears, confirming deprotonation and coordination through the phenolic oxygen. The C–O stretching frequency shifts to a higher wavenumber due to the formation of the metal–oxygen bond. Meanwhile, the C=N or aromatic ring vibrations of the quinoline moiety shift to lower frequencies, further indicating coordination via the nitrogen atom. As with the coumarin–pyridine ligand, new bands in the region of 400–600 cm^{-1} appear, representing the metal–ligand (Nd–O and Nd–N) stretching vibrations. These IR spectral changes collectively confirm the successful coordination of both ligands to the neodymium (III) center.

Table 4. Selected IR data (cm^{-1}) for the Nd (III) complexes.

Complex	υ (CH=N)	υ (CH=O)	υ (Nd – O)	υ (Nd – N)
C_1	1542	1647	531	453
C_2	1532	1641	528	438
C_3	1540	1632	529	430
C_4	1530	1630	532	432

Thermal Analysis of The Synthesized Complexes

Table 5. TGA decomposition analytical data of complexes.

Complex	TG range (C)	Mass loss (%) Obs. (cal.)	Assignment
C_1	30 – 150	03.50	Loss of 2lattice water
	150 – 300	36.80	Loss of CQ ligand (including loss of coordinated Cl^-)
	300 – 500	47.65	Loss of ligand L_1
	500 – 700	12.05	Formation of Nd_2O_3
C_2	30 – 150	3.36	Loss of lattice water
	150 – 300	35.14	Loss of CQ + 2 Cl atoms
	300 – 500	49.67	Loss of Ligand L_2
	500 – 700	11.83	Residue of Nd_2O_3

C_3	30 – 150	3.31	Loss of 2 lattice water
	150 – 300	34.62	Loss of CQ ligand + 2Cl atom
	300 – 500	50.42	Loss of L_3 ligand
	500 – 700	11.65	Residue of Nd_2O_3
C_4	30 – 150	3.17	Loss of 2 lattice water
	150 – 300	40.18	Loss of CQ ligand + 1Br atom + 2Cl atom
	300 – 500	52.47	Loss of L_3 ligand
	500 – 700	4.18	Residue of Nd_2O_3

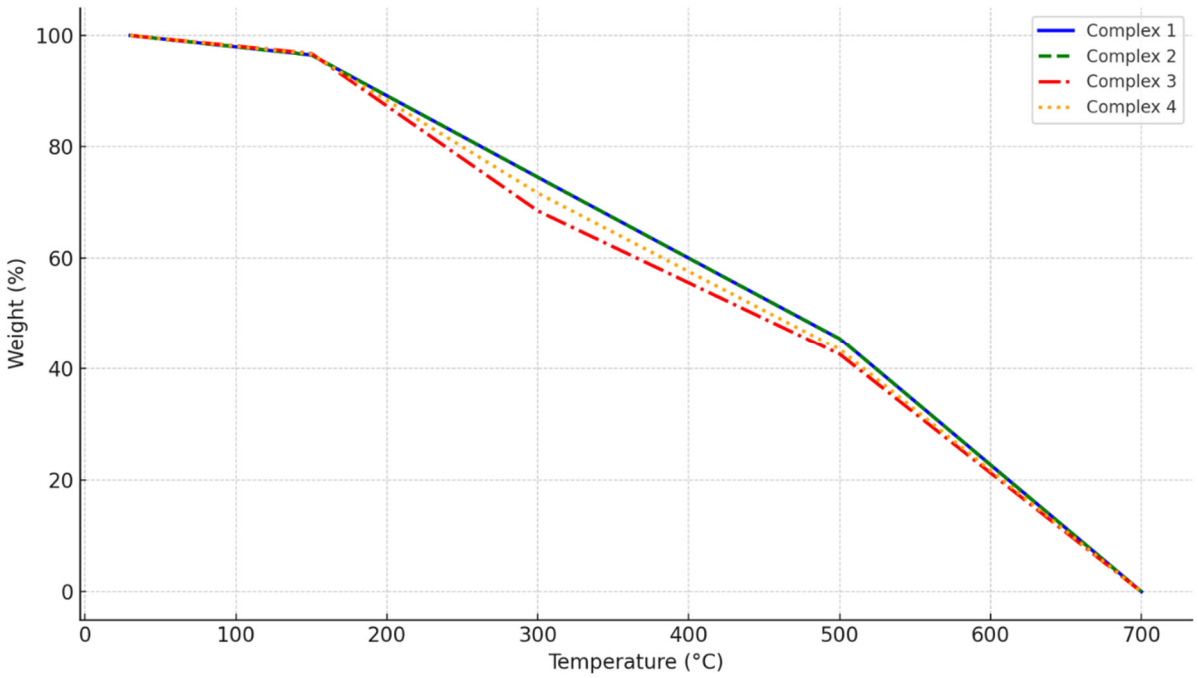

Figure 1. TGA curve of complexes (L_1 – L_4).

Figures 1 depict the TG curves for Nd(III) complexes C_1 – C_4, while Table 5 presents the thermal data gleaned from the thermal curves, aligning with other investigations. The utilization of thermogravimetric analysis in assessing mixed-ligand complexes can furnish valuable insights into their thermal stability and decomposition processes. This knowledge is instrumental in comprehending the mechanisms underlying the decomposition and optimizing synthesis and storage conditions for such complexes.

Mass Spectra

The mass spectra indicates molecular ion peaks for complexes C_1 through C_4, appearing at m/z = 1055, 1069, 1085, and 1098 observed. Utilizing these peaks, alongside the mass spectrum for complex I depicted in Figure 2, confirms the molecular formulas of the complexes, devoid of water of crystallization. Moreover, the fragmentation patterns unveil valuable structural insights into the complexes. By analysing these fragmentation products, the positioning of ligands on the copper atom and the relative strengths of metal-ligand bonds can be discerned. Furthermore, the relative intensities of these products offer information on complex stability and the energetics of fragmentation, aiding in comprehending the behaviour and properties of the complexes across diverse applications.

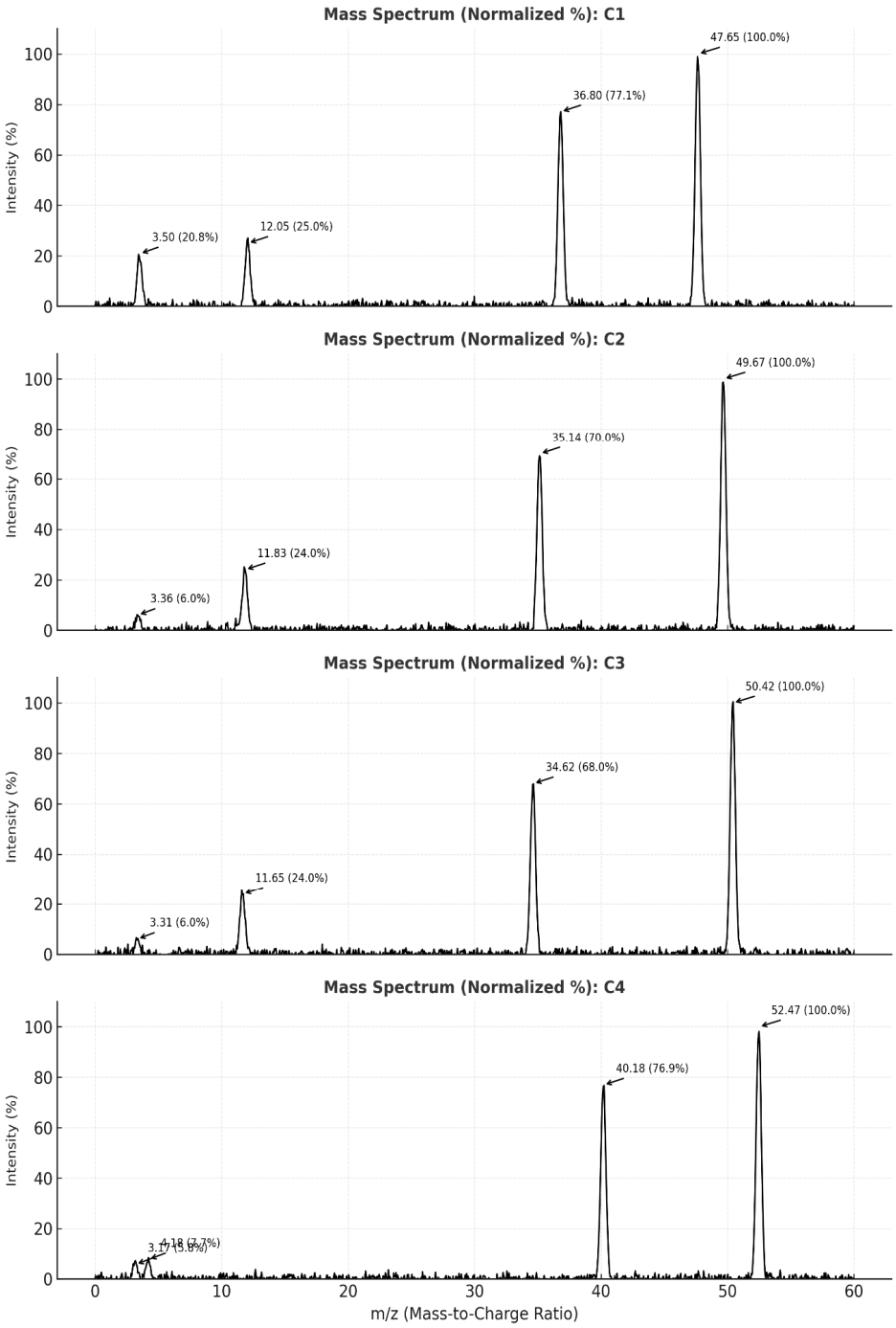

Figure 2. Mass spectral data of complexes.

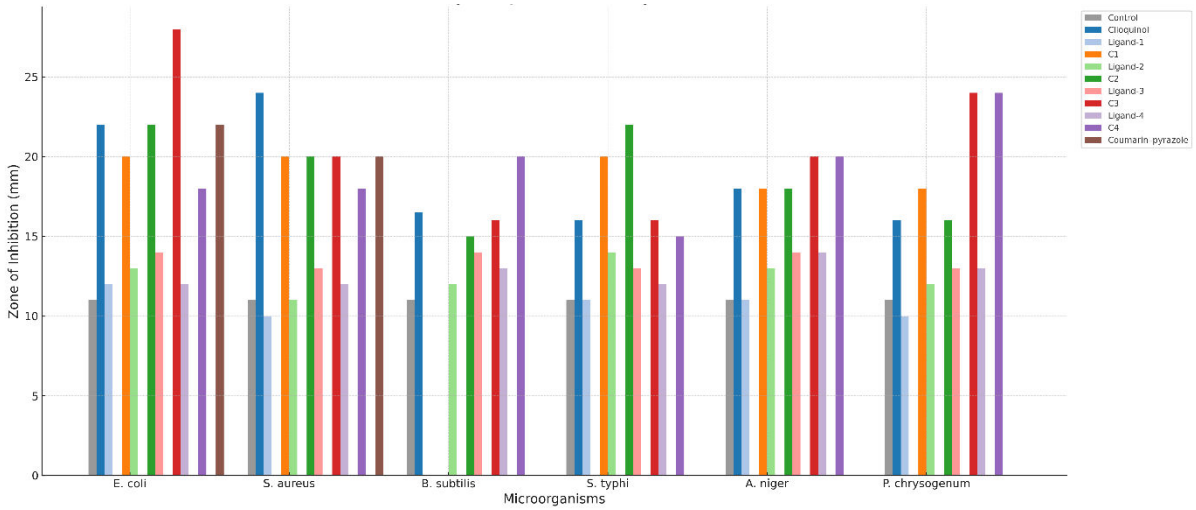

Figure 3. Anti – microbial Activity of Complexes.

The antimicrobial activity of the synthesized ligands, their neodymium (III) complexes (C1–C4), and the coumarin–pyrazole complex was assessed using the agar well diffusion method. Stock solutions (10 mg/mL) were prepared by dissolving the compounds in DMSO and diluting them with double distilled water. All solutions were sterilized by filtration through a 0.22 µm membrane.

Sterile nutrient agar (LB for *bacteria*, PDA for *fungi*) was prepared and autoclaved at 121 °C for 20 minutes. The microbial strains (*E. coli*, *S. aureus*, *B. subtilis*, *S. typhi*, *A. niger*, and *P. chrysogenum*) were activated in suitable liquid media and incubated until they reached the logarithmic growth phase.

Sterile Petri dishes were poured with the agar, and after solidification, they were inoculated with standardized microbial suspensions. Wells of 6 mm diameter were bored into the agar, and 100 µL of each test compound was introduced into the respective wells. Control wells contained only DMSO with water, while clioquinol and fluconazole served as the standard antibacterial and antifungal agents, respectively.

Plates were incubated at 37 °C for 24 hours for bacterial strains and at 28 °C for 48 hours for fungal strains. Zones of inhibition were measured in millimetres, and results were averaged from triplicate experiments. The result is detailed in Table 6 and Figure 3.

Table 6. Antibacterial Activity Data of Synthesized Ligands and Complexes.

Organism	Control	CQ	L_1	C_1	L_2	C_2	L_3	C_3	L_4	C_4
Escherichia coli	10 – 12	22	12	20	13	22	14	28	12	18
Staphylococcus aureus	10 – 12	24	10	20	11	20	13	20	12	18
Bacillus subtilis	10 – 12	16.5	-	-	12	15	14	16	13	20
Salmonella typhi	10 – 12	16	≥11	≥20	14	22	13	16	12	15
Aspergillus Niger	10 – 12	18	11	18	13	18	14	20	14	20
Penicillium chrysogenum	10 – 12	16	10	16	12	16	13	24	13	24
Aspergillus flavus	10 – 12	-	-	-	-	-	-	-	-	-

4. DISCUSSION

The antimicrobial activities of the synthesized coumarin–pyrazole ligands (L_1–L_4) and their corresponding neodymium (III) complexes (C_1–C_4) were evaluated against both Gram-positive and Gram-negative bacterial strains (*Escherichia coli*, *Staphylococcus aureus*, *Bacillus subtilis*, and *Salmonella typhi*) as well as fungal species (*Aspergillus niger*, *Penicillium chrysogenum*, and *Aspergillus flavus*). The results, expressed as the diameter of the inhibition zones (mm), are summarized in Table 6.

In general, the neodymium (III) complexes exhibited greater antimicrobial activity than the corresponding free ligands. The enhanced activity may be attributed to chelation, which reduces the polarity of the metal ion through partial sharing of its positive charge with donor atoms and delocalization of π-electrons within the chelate ring. This increases the lipophilicity of the complexes, facilitating their penetration through the lipid layers of microbial cell membranes and improving biological efficacy.

Among the bacterial strains, *E. coli* and *S. typhi* showed the highest sensitivity toward the complexes, particularly C_3 and C_2, with inhibition zones reaching 28 mm and 22 mm, respectively. The Gram-positive strains *S. aureus* and *B. subtilis* also showed moderate inhibition, while *A. flavus* exhibited negligible activity against all ligands and complexes. The antifungal evaluation revealed that *A. niger* and *P. chrysogenum* were moderately sensitive, with the most active complexes again being C_3 and C_4, suggesting that substitution on the coumarin–pyrazole framework and mixed coordination with clioquinol enhance biological performance.

These findings clearly demonstrate that the incorporation of neodymium (III) into the coumarin–pyrazole–clioquinol framework plays a crucial role in modulating antimicrobial potency. The results are consistent with previous reports on lanthanide complexes, where chelation markedly increases biological activity compared with uncoordinated ligands.

5. CONCLUSION

A new series of neodymium(III) complexes with coumarin–pyrazole derivatives and clioquinol as mixed ligands was successfully synthesized. Spectroscopic and magnetic studies confirmed 8-coordinate geometry around the Nd^{3+} center, with coordination via azomethine nitrogen, carbonyl oxygen, and phenolic oxygen atoms. The complexes exhibited good solubility in DMSO and DMF and showed enhanced antimicrobial activity compared with the free ligands, particularly against *E. coli*, *S. typhi*, *A. niger*, and *P. chrysogenum*, with C_2 and C_3 being the most active. The increased activity is attributed to chelation, which enhances lipophilicity and facilitates cell membrane penetration, highlighting their potential as antimicrobial agents**.**

Acknowledgment

I would like to extend my heartfelt appreciation to Navjivan Science College, Dahod, for their generous provision of laboratory facilities. Access to advanced equipment and resources has significantly facilitated the progress of my research and experimental work. The support and assistance from the college staff have been invaluable, and the conducive environment has fostered a space for learning and innovation. I am profoundly grateful for the opportunity to utilize such facilities, which have been instrumental in achieving the objectives of my scientific endeavours. Thank you, Navjivan Science College, for your commitment to nurturing the scientific community and for your pivotal role in facilitating academic growth.

References

[1] Boeck, F., Blazejak, M.,Anneser, M. R., & Hintermann, L. (2012).Cyclization of ortho-hydroxycinnamates to coumarins under mild conditions: A nucleophilic organocatalysis approach. *Beilstein Journal of Organic Chemistry, 8*, 1630–1636. https://doi.org/10.3762/bjoc.8.186

[2] Kumari, S., Sharma, A., & Yadav, S. (2023). Pharmacological potential of coumarin-based derivatives: A comprehensive brief review. *Oriental Journal of Chemistry, 39*(3), 568–576. https://doi.org/10.13005/ojc/390304

[3] Sharma, P. (2017). *Natural coumarin derivatives activating Nrf2 signaling pathway as intestinal anti-inflammatory agents* [Book chapter]. In *Recent Advances in Natural Products Research* (pp. 45–68). Springer.

[4] Brown, K. (2009). *Coumarin: A natural solution for alleviating inflammatory disorders* [Book]. Wiley-VCH.

[5] Yadav, A. K., Shrestha, R. M., & Yadav, P. N. (2024). Anticancer mechanism of coumarin-based derivatives.*European Journal of Medicinal Chemistry, 267*, 116179. https://doi.org/10.1016/j.ejmech.2024.116179

[6] Patel, H., & Gupta, S. (2011). *Synthetic heterocyclic coumarin modifications* [Book chapter]. In *Advances in Heterocyclic Chemistry* (Vol. 17, pp. 101–130). Academic Press.

[7] Tiwari, A., Singh, R., & Mehta, P. (2014). *Therapeutic heterocyclic fusion review* [Book chapter]. In *Heterocyclic Chemistry in Drug Discovery* (pp. 223–250). Elsevier.

[8] Ding, W. Q., Liu, B., Vaught, J. L., Yamauchi, H., & Lind, S. E. (2005). Anticancer activity of the antibiotic clioquinol. *Cancer Research, 65*(8), 3389–3395. https://doi.org/10.1158/0008-5472.CAN-04-3577

[9] Vašák, M., et al. (2005). Stoichiometry and conditional stability constants of Cu(II)- or Zn(II)-clioquinol complexes: Implications for Alzheimer's and Huntington's disease therapy. *NeuroToxicology*.

[10] Opazo, C., et al. (2006). Radio iodinated clioquinol as a biomarker for β-amyloid: Zn^{2+} complexes in Alzheimer's disease. *Aging Cell, 5*(1), 69–79. https://doi.org/10.1111/j.1474-9726.2006.00196.x

[11] Pushpa Nathan, M., et al. (2020). Clioquinol metal complexes in inorganic chemistry. *Inorganica Chimica Acta, 504*, 119466.

[12] Salehi, S., et al. (2019). Biological activities of clioquinol-based metal complexes. *Journal of Inorganic Biochemistry, 197*, 110697.

[13] Huang, X., et al. (2019). Pharmacokinetic modulation in clioquinol-metal complexes. *Molecular Pharmaceutics, 16*, 2886–2897.

[14] Abdel-Fatah, N. A., El-Bindary, A. A., & El-Morshedy, R. M. (2017). Nd(III) complexes with Schiff base ligands: Synthesis, characterization and antimicrobial 12.studies. *Journal of Chemical and Pharmaceutical Research*, 9(4), 197–203. *(DOI not available; accessible via journal website: jocpr.com)*

[15] Taha, Z. A., Hijazi, A. K., & Momani, W. A. (2020). Lanthanide complexes of the tridentate Schiff base ligand salicylaldehyde-2-picolinoylhydrazone: Synthesis, biological activities, and catalytic oxidation. *Journal of Molecular Structure*, Article ID 791219. https://doi.org/10.1155/2012/791219

[16] Alnufaie, R., Al-Majid, A. M., Al-Karagoly, H., & Majrashi, M. (2020). Synthesis and antimicrobial studies of coumarin-substituted pyrazole derivatives as potent anti-Staphylococcus aureus agents. *Molecules*, 25(12), 2758. https://doi.org/10.3390/molecules25122758

[17] Sayed, M. T., Abdou, W. M., El-Sayed, A. A., & El-Kashif, A. (2023). Synthesis and antimicrobial activity of new series of thiazoles, pyridines and pyrazoles based on coumarin moiety. *Scientific Reports*, 13, 9912. https://doi.org/10.1038/s41598-023-36705-0